Nucleotide–amino acid interactions in the L-His–IMP·MeOH·H2O complex

Katarzyna Ślepokura* and Rafał Petrus

Faculty of Chemistry, University of Wrocław, 14 Joliot-Curie Street, 50-383 Wrocław, Poland

Correspondence e-mail: slep@eto.wchuwr.pl

In the crystal structure of the methanol-solvated mono-hydrated complex of L-histidine (His) with inosine 5′-monophosphate (IMP), namely L-histidinium inosine-5′-phosphate methanol solvate monohydrate, $C_6H_{10}N_3O_2^+$·$C_{10}H_{12}N_4O_8P^-$·CH_3OH·H_2O, most of the interactions between IMP anions (anti/C3′-endo/gauche–gauche conformers) are realized between the riboses and hypoxanthine bases in a trans sugar-edge/sugar-edge geometry, and between the phosphate groups. The base Watson–Crick edge is involved in additional methanol-mediated IMP···MeOH···IMP contacts. Specific and nonspecific nucleotide–amino acid (IMP···His) interactions engage the Hoogsteen edges of the base and phosphate group, respectively. Additional stabilization of His···IMP contacts is provided by π–π stacking between the imidazolium ring of His and the hypoxanthine base of IMP. The results may indicate the possible recognition mechanism between His and IMP.

Comment

Specific protein–nucleotide/nucleic acid interactions are realized mainly *via* direct hydrogen bonds between the nucleotide base and amino acid side chain, hydrophobic interactions, and π–π stacking between the base and aromatic side chain (Rice & Correll, 2008). For base contacts, significant amino acid–base-type correlations have been revealed, with the most obvious being the arginine–guanine pair (Luscombe *et al.*, 2001; Hoffman *et al.*, 2004). Inspection of DNA–protein complexes has also shown a histidine–guanine preference (Luscombe *et al.*, 2001). In protein–DNA complexes, the main specificity is ascribed to the major rather than the minor groove. In protein–RNA, as well as in protein–nucleotide recognition, the different edges of a base may play a similar role in protein binding. According to the descriptive nomenclature based on geometry, introduced by Leontis & Westhof (2001) for classification of non-Watson–Crick RNA base pairing, three distinct edges in the nucleotide base may be distinguished: the Watson–Crick edge, the Hoogsteen edge (equivalent to the B-DNA major groove and RNA A-type helix deep groove), and the sugar edge (which includes the 2′-OH group and is equivalent to the B-DNA minor groove and RNA shallow groove).

(I)
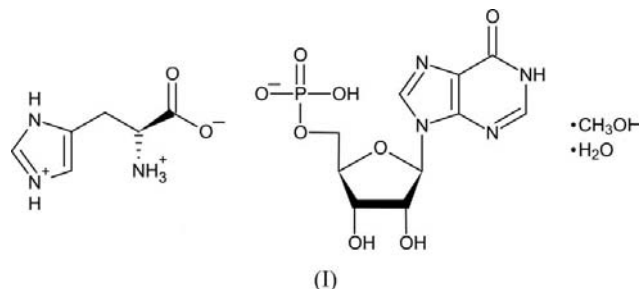
We believe that the high-resolution crystal structures of amino acid–nucleotide complexes could be a reliable and informative tool in the investigation of protein–nucleic acid interactions and their manner of recognition. We have therefore undertaken the synthesis and structural analysis of the title L-His–IMP·MeOH·H2O complex, (I), presented here, which reveals both the specific and the nonspecific interactions of L-histidine (His) with inosine 5′-monophosphate (IMP), commonly found in tRNA's nucleotide. The conformation and binding mode of IMP are compared with those found in three other amino acid–IMP complexes deposited in the Cambridge Structural Database (CSD; Allen, 2002) and in high-resolution protein–IMP complexes deposited in the Protein Data Bank (PDB; Berman *et al.*, 2000). The three isomorphous complexes of IMP with L-Ser (CSD refcode ZUWQEN; Mukhopadhyay *et al.*, 1995), L-Glu (QUSMIA; Bhattacharya *et al.*, 2000) and L-Gln (LIRQUY; Bera *et al.*, 1999), along with two complexes of N^7-methylguanosine 5′-monophosphate (m⁷GMP) with L-Phe and Trp–Glu [DUMJEA10 (Ishida *et al.*, 1988) and SEKXIP10 (Ishida *et al.*, 1991), respectively], are the only examples of amino acid/oligopeptide–nucleotide complexes reported so far (not counting five coordination compounds containing cobalt or platinum cations interfering with the amino acid–nucleotide interactions). Unfortunately, the quality of the data for the previously reported complexes is not satisfactory. In addition, in the highly hydrated IMP–Ser/Glu/Gln complexes, no direct specific nucleobase–amino acid functional site interactions can be observed.

The asymmetric unit of (I) consists of an IMP monoanion, a His cation and two solvent molecules (methanol and water), as shown in Fig. 1. The nucleotide adopts an *anti* conformation, typical for both free and amino acid-complexed IMP, about the N-glycosidic C1′—N9 bond (χ_{CN} O4′—C1′—N9—C4 close to a common value of 140°; Table 1), and also a typical *gauche–gauche* conformation about the C4′—C5′ bond. The relative orientation of the hypoxanthine (Hyp) base and ester atom O5′ is stabilized by an intramolecular C8—H8···O5′ hydrogen bond (Table 2), shown as a dashed line in Fig. 1.

Interestingly, while the high-resolution crystal structures of protein-bound IMP [RNase A–IMP complex, PDB ID 1Z6D (Hatzopoulos *et al.*, 2005), and NTPase–IMP complex, 2DVN (Lokanath *et al.*, 2008)] reveal a slight preference for *anti* over *syn* conformations about the glycosidic bond, the same structures show that the IMP molecules, upon binding to the
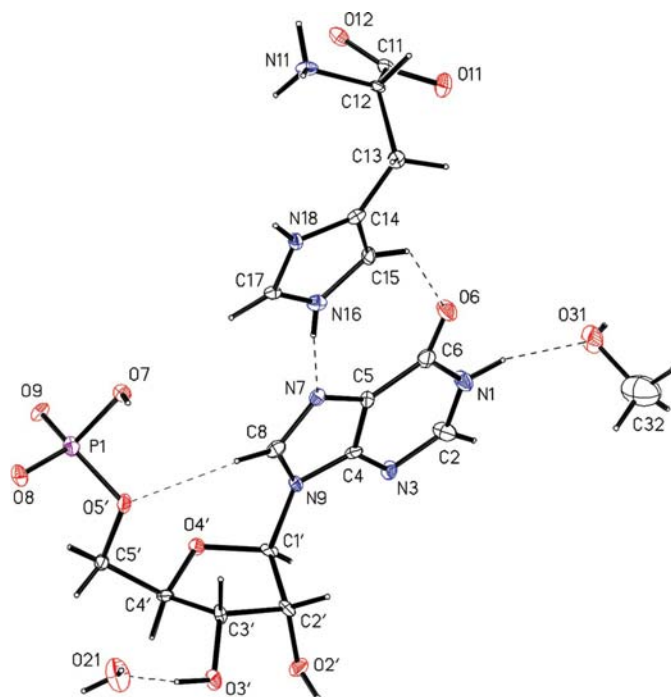
organic compounds

Figure 1
The structures and atom-numbering schemes for the His cation, IMP anion and solvent molecules joined by hydrogen bonds (dashed lines) in the asymmetric unit of (I). The intramolecular C8—H8···O5′ contact, stabilizing the IMP structure, is also shown. Displacement ellipsoids are drawn at the 30% probability level and H atoms are shown as small spheres of arbitrary radii.

protein active site, adopt diverse conformations about the C4′—C5′ bond, *i.e. gauche–trans*, *trans–gauche* and *gauche–gauche*.

The nucleotide ribose ring in (I) is puckered in an envelope C3′-*endo* (^3E) manner, as confirmed by the pseudorotation parameters (Rao *et al.*, 1981) $P = 13.9 (5)°$ and $\tau_m = 33.7 (3)°$ (reference bond C2′—C3′), as well as by the Cremer & Pople (1975) puckering parameters $q_2 = 0.328 (6)$ Å and $\varphi_2 = 283 (1)°$. The envelope ^3E conformation is one of two typically observed in free IMP and other free and protein-bound nucleotides (Allen, 2002; Moodie & Thornton, 1993), but was not observed in the previously reported amino acid–nucleotide (both IMP and m^{7}GMP) complexes, in which C2′-*endo* (^2E) puckering is the most common. Similarly, the ribose in protein-bound IMP does not reveal any conformational preference and is found in various puckering conformations, *i.e.* C2′-*endo* (^2E), C2′-*exo* (E_2), C1′-*endo* (^1E), C3′-*endo* (^3E) and C4′-*exo* (E_4).

As seen from the β torsion angle (P1—O5′—C5′—C4′; Table 1), the phosphate group of the inosine nucleotide of (I) is oriented in an antiperiplanar manner relative to the ribose ring, which is also a characteristic of amino acid-complexed IMP, but not the only preferred conformation for protein-bound IMP and other nucleotides (Moodie & Thornton, 1993; Berman *et al.*, 2000). The orientation of the terminal phosphate O atoms relative to atom C5′, with the two O atoms (O8 and O9) being in ±*sc* positions and the third (hydroxy atom O7) in an *ap* position, is typical for organic phosphate

monoesters. However, the location of the H atom in the phosphate group at the antiperiplanar O atom is not often observed in monoanionic phosphate esters. The geometry of the monoionized IMP phosphate group reveals a significant deformation from the ideal tetrahedral shape (Table 1), with the O7—P1—O5′ angle, formed by the ester and the hydroxyl O$_{ap}$ atom, being the smallest of all the phosphate angles (∼100°) and the remaining O—P—O angles being in the range 107–114°. The value of the O7—P1—O5′ angle correlates with the P1—O5′ and P1—O7 bond lengths, being significantly longer than the other P—O bonds (Table 1).

The His cation of (I), with the carboxyl group deprotonated and both amino atom N11 and imidazole atom N16 (N$^\varepsilon$) protonated, reveals a perpendicular orientation of the imidazolium ring and C$^\alpha$12—C$^\beta$13—C$^\gamma$14 fragment, which is reflected in the interplanar angle of 86.8 (4)° and in the χ^2 (C$^\alpha$12—C$^\beta$13—C$^\gamma$14—N$^\delta$18/C$^\delta$15) torsion angles, which are close to ±90° (Table 1). These, in combination with a χ^1 (N11—C$^\alpha$12—C$^\beta$13—C$^\gamma$14) angle close to 65°, indicate the location of protonated atoms N11 and N18 (N$^\delta$) on the same side of the His cation, as shown in Fig. 1, which plays a role in the His···IMP interactions, as will be discussed later.

Among all the intermolecular interactions observed in the crystal structure of (I) (Table 2), three general types of direct contacts may be distinguished: (*a*) His···His interactions between adjacent His cations, (*b*) IMP···IMP interactions between nucleotide anions, and (*c*) His···IMP interactions, crucial to the amino acid–nucleotide recognition process. In addition, indirect solvent-mediated hydrogen bonds are present.

Both His···His and IMP···IMP interactions arrange adjacent His cations or IMP anions (related by a 2$_1$ axis and a direct *b*-axis translation) into infinite helices running down the *b* axis, as shown in Fig. 2. Within the His helix, the ammonium and carboxylate groups of adjacent His cations interact with each other *via* N11—H11*C*···O12^{viii} hydrogen bonds of a salt-bridge type [symmetry code: (viii) $-x + 2, y + \frac{1}{2}, -z + 1$]. As a result, the His functional groups (protonated imidazole rings) are exposed outside the helix, which enables the specific amino acid–nucleotide interactions. The structure of the His helix is additionally stabilized by interactions between adjacent cations related by a direct *b*-axis translation (Fig. 2*a* and Table 2), *viz.* unusually short C—H···O hydrogen bonds [C$^\alpha$12—H12···O12^i; symmetry code: (i) $x, y + 1, z$] and C—H···π interactions [C$^\beta$13—H13*B*···Cg1^i (Cg1 is the centroid of the protonated imidazole ring of the His cation), with a perpendicular H13*B*···ring^i plane distance of 2.70 Å, an H13*B*···Cg^i distance of 2.97 Å and a C13—H13*B*···Cg1^i angle of 146°].

Similarly, in the IMP helix, a direct *b*-axis translation and strong phosphate–phosphate O7—H7···O9^i hydrogen bonds, along with close sugar–sugar C—H···O contacts and possible base–base C=O···π interactions [C6=O6···Cg2^i (Cg2 is the centroid of the N1–C6 ring), with a perpendicular O6···ring^i distance of 3.289 Å, an O6···Cg2^i distance of 3.488 (5) Å and a C6=O6···Cg2^i angle of 101.0 (4)°], generate infinite chains of IMP anions running down the *b* axis. The mutual orienta-
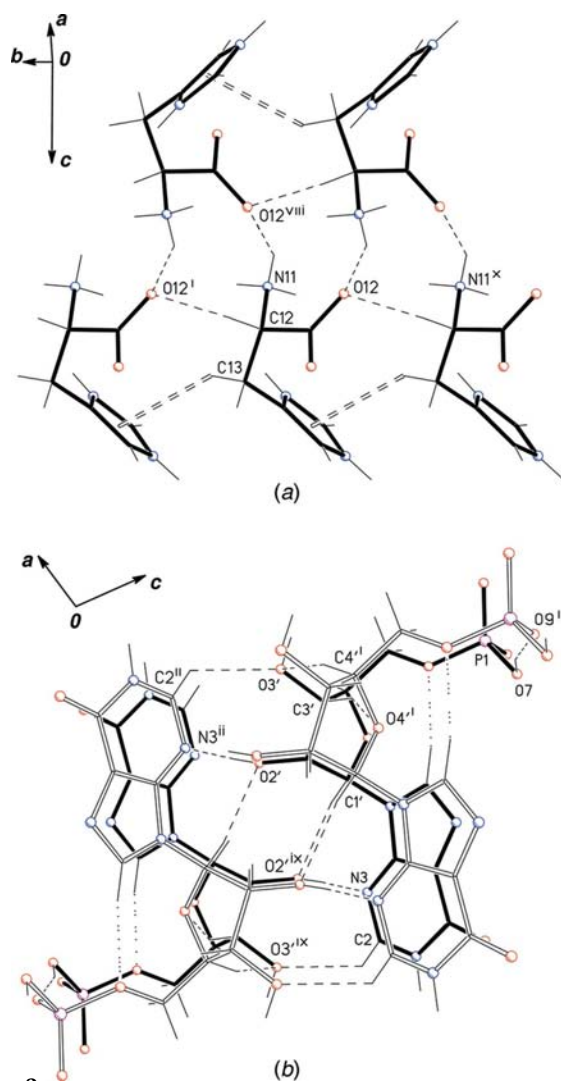
Figure 2
The arrangement of (a) the histidinium cations and (b) the IMP anions within the separate helices running down the b axis. Intermolecular His···His [in (a)] and IMP···IMP [in (b)] interactions are shown with dashed lines, C—H···π interactions with dashed open lines and intramolecular C8—H8···O5′ interactions with dotted lines. (Symmetry codes are as given in Table 2.)

tion and interactions between two parallel chains related by the action of a 2_1 screw axis result in the helices having the IMP anions arranged in a *trans* manner and pointing their sugar edges towards each other, as shown in Fig. 2(b). Therefore, most of the intra-helical IMP···IMP interactions (besides those between the phosphate groups) are realized between the riboses and the hypoxanthine (Hyp) bases in a *trans* sugar-edge/sugar-edge geometry (Leontis & Westhof, 2001). These are sugar–base [O2′—H2′···N3(Hyp)]^{ii} and C2(Hyp)—H2···O3′^{ix}; symmetry codes: (ii) $-x + 1$, $y + \frac{1}{2}$, $-z + 2$; (ix) $-x + 1$, $y - \frac{1}{2}$, $-z + 2$] and sugar–sugar close C—H···O contacts, which also involve ribose atom O3′ (in polynucleotides, this atom constitutes the nucleic acid backbone and is thus not considered as a sugar-edge atom). The Watson–Crick edges are engaged in methanol-mediated IMP···MeOH···IMP interactions involving hypoxanthine atoms N1 and O6, *viz.* N1—H1···O31—H31···O6^{v} [symmetry code: (v)
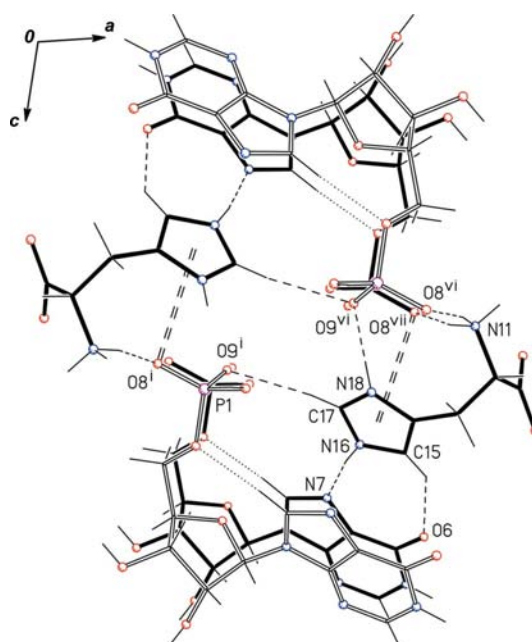
Figure 3
The specific and nonspecific His···IMP hydrogen bonds (dashed lines) observed in (I). Close P—O···π(His) and intramolecular C8—H8···O5′ contacts are shown with double dashed and dotted lines, respectively. (Symmetry codes are as given in Table 2.)

$-x + 2$, $y - \frac{1}{2}$, $-z + 2$]. In the previously reported IMP complexes, the IMP···IMP contacts, seeming to be genuinely predominant, were realized mainly *via* phosphate–ribose interactions involving both atoms O2′ and O3′, and *via* N1(Hyp)···phosphate contacts, which are additionally possible in Ser–IMP and Gln–IMP, but not in Glu–IMP.

Finally, the nucleotide Hoogsteen edge, commonly used in protein–nucleic acid recognition, is also involved in amino acid–nucleotide (His···IMP) interactions in (I). As shown in Figs. 1 and 3, the histidine side-chain–Hyp base recognition is realized *via* specific hydrogen bonds utilizing both Hyp atoms N7 and O6, *i.e.* N$^{\varepsilon}$16—H16···N7(Hyp) and C$^{\delta}$15—H15···O6(Hyp) (Table 2). In DNA–protein complexes, histidine has been shown to prefer interactions with guanine (Luscombe *et al.*, 2001), which is a 2-amino derivative of hypoxanthine and thus has the same Hoogsteen edge crucial for protein–DNA recognition. Direct amino acid side-chain–Hyp interactions were not observed in the other IMP–amino acid complexes, but they may be analysed in macromolecular protein–IMP complexes. Hyp atom N7 in one of the IMP molecules in the complexes RNase A–IMP (Hatzopoulos *et al.*, 2005) and NTPase–IMP (Lokanath *et al.*, 2008) is involved in such hydrogen bonding to O$^{\gamma}$(Thr) and N$^{\eta 2}$(Arg), respectively. In the NTPase–IMP complex, the Hyp bases interact *via* O6···N$^{\zeta}$(Lys), O6···N$^{\varepsilon}$(His) and O6···N$^{\eta 1}$(Arg) contacts. In protein–IMP complexes, N1(Hyp)···amino acid side-chain interactions are also commonly observed. However, in the L-His–IMP complex presented here, this atom is involved in IMP···MeOH···IMP interactions, and therefore does not bind His at all.

The nucleotide anionic phosphate group in the present L-His–IMP complex, (I), accepts four additional nonspecific
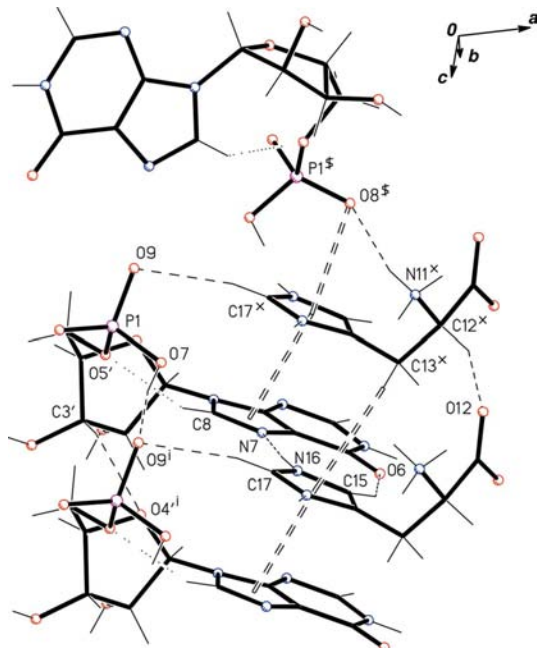
Figure 4
L-His cations and IMP anions interacting *via* π–π stacking and close P—O···π(His) contacts (dashed open lines). His···His C—H···π interactions (dashed open lines), and inter- and intramolecular hydrogen bonds (dashed and dotted lines, respectively) are also shown. [Symmetry codes are as given in Table 2; additionally: ($) $-x + 1, y - \frac{1}{2}, -z + 1$.]

N/C—H···O hydrogen bonds from three different His cations, two of which are bound in a monodentate manner (*via* the NH_3^+ group or imidazolium ring) and the third in a bidentate manner *via* both ammonium atom N11 and imidazolium atom N18 (N^δ) (Fig. 3). The latter is facilitated by the specific His conformation with both atoms N11 and N18 located on the same side, as discussed above. Phosphate–His hydrogen bonds are also observed in the RNase–IMP complex, where the phosphate group of one of the three bound IMP molecules interacts with atoms N^δ and N^ε of two different His residues from the catalytic triad.

In the current L-His–IMP complex, nucleotide ribose atom O3′ is involved in water-mediated IMP···H_2O···His interactions, *viz.* O3′—H3′···O21—H21A···O11^{iii} and O3′—H3′···O21—H21B···O11^{iv} [symmetry codes: (iii) $x - 1, y - 1, z$; (iv) $x - 1, y, z$]. Additional stabilization of the His···IMP contacts is provided by π–π stacking of the cation···π type, formed between the centroid Cg1 of the protonated imidazole ring of the His cation and the Hyp base of the IMP anion [centroid–centroid distance = 3.693 (4) Å], as shown in Fig. 4. A close P1—O8···Cg1$^{\$}$ contact, which can be classified as a lone-pair···π interaction, is also observed, with a perpendicular O8···ring$^{\$}$ plane distance of 3.24 Å, an O8···Cg1$^{\$}$ distance of 3.567 (4) Å and a P1—O8···Cg1$^{\$}$ angle of 105.1 (2)° [symmetry code: ($) $-x + 1, y - \frac{1}{2}, -z + 1$] (Fig. 4).

Experimental

An MeOH/water solution (1:10 *v/v*) containing a 1:1 or 1:2 molar ratio of inosine 5′-phosphate disodium salt (IMPNa$_2$; Sigma–Aldrich) and L-histidine hydrochloride (L-His·HCl; Chemapol) was heated at

333 K for 15 min. Slow evaporation of the resulting solution at room temperature gave small needle-shaped, mostly twinned, crystals of L-His–IMP·MeOH·H$_2$O, (I).

Table 1
Selected geometric parameters (Å, °).

P1—O5′	1.590 (3)	O6—C6	1.240 (6)
P1—O7	1.576 (3)	O11—C11	1.256 (5)
P1—O8	1.501 (3)	O12—C11	1.243 (6)
P1—O9	1.519 (4)		
O5′—P1—O7	100.3 (2)	O7—P1—O8	114.3 (2)
O5′—P1—O8	110.6 (2)	O7—P1—O9	107.0 (2)
O5′—P1—O9	109.6 (2)	O8—P1—O9	114.1 (2)
O7—P1—O5′—C5′	−175.2 (4)	O11—C11—C12—N11	−175.9 (4)
O8—P1—O5′—C5′	63.8 (4)	O11—C11—C12—C13	−46.9 (6)
O9—P1—O5′—C5′	−62.9 (4)	N11—C12—C13—C14	64.8 (6)
C4—N9—C1′—O4′	−139.2 (5)	C11—C12—C13—C14	−63.4 (6)
P1—O5′—C5′—C4′	165.4 (3)	C12—C13—C14—N18	−87.7 (7)
O4′—C4′—C5′—O5′	−63.0 (5)	C12—C13—C14—C15	93.8 (7)
C3′—C4′—C5′—O5′	54.2 (6)		

Table 2
Hydrogen-bond geometry (Å, °).

D—H···A	D—H	H···A	D···A	D—H···A
O7—H7···O9^i	0.84	1.74	2.549 (5)	162
O2′—H2′···N3^{ii}	0.84	2.04	2.863 (6)	165
O3′—H3′···O21	0.84	1.91	2.707 (6)	157
O21—H21A···O11^{iii}	0.80 (6)	2.03 (7)	2.805 (6)	164 (7)
O21—H21B···O11^{iv}	0.73 (7)	2.15 (7)	2.824 (6)	153 (8)
O31—H31···O6^v	0.84	1.92	2.716 (5)	158
N1—H1···O31	0.88	1.84	2.695 (6)	165
N11—H11A···O8^{vi}	0.91	1.99	2.891 (5)	168
N11—H11B···O8^{vii}	0.91	1.97	2.856 (6)	164
N11—H11C···O12^{viii}	0.91	1.95	2.737 (5)	144
N16—H16···N7	0.88	1.89	2.767 (6)	171
N18—H18···O9^{vi}	0.88	1.87	2.716 (5)	161
C1′—H1′···O2^{ix}	1.00	2.70	3.683 (6)	168
C3′—H3′A···O4′^{i}	1.00	2.49	3.340 (7)	142
C4′—H4′···O3′^{x}	1.00	2.70	3.597 (7)	150
C2—H2···O3′^{ix}	0.95	2.38	3.064 (7)	128
C8—H8···O5′	0.95	2.34	3.179 (6)	147
C12—H12···O12^i	1.00	2.08	2.964 (7)	146
C15—H15···O6	0.95	2.47	3.221 (7)	136
C17—H17···O9^i	0.95	2.45	3.385 (6)	168
C32—H32B···O11^v	0.98	2.47	3.183 (8)	130
C32—H32C···O3′^{vii}	0.98	2.55	3.467 (8)	156

Symmetry codes: (i) $x, y + 1, z$; (ii) $-x + 1, y + \frac{1}{2}, -z + 2$; (iii) $x - 1, y - 1, z$; (iv) $x - 1, y, z$; (v) $-x + 2, y - \frac{1}{2}, -z + 2$; (vi) $-x + 1, y + \frac{3}{2}, -z + 1$; (vii) $-x + 1, y + \frac{1}{2}, -z + 1$; (viii) $-x + 2, y + \frac{1}{2}, -z + 1$; (ix) $-x + 1, y - \frac{1}{2}, -z + 2$; (x) $x, y - 1, z$.

Refinement

$R[F^2 > 2\sigma(F^2)] = 0.052$
$wR(F^2) = 0.070$
$S = 0.77$
4289 reflections
346 parameters
1 restraint

H atoms treated by a mixture of independent and constrained refinement
$\Delta\rho_{max} = 0.34$ e Å^{-3}
$\Delta\rho_{min} = -0.38$ e Å^{-3}
Absolute structure: Flack (1983), with 1785 Friedel pairs
Flack parameter: -0.04 (18)

All H atoms were found in difference Fourier maps. In the final refinement cycles, all except for water-bonded H atoms were positioned geometrically and treated as riding atoms, with C—H = 0.95–1.00 Å, N—H = 0.88–0.91 Å and O—H = 0.84 Å, and with $U_{iso}(H) = 1.2U_{eq}(C,Nsp^2)$ or $1.5U_{eq}(O,Nsp^3)$. The positions of the water H atoms were refined with $U_{iso}(H) = 1.5U_{eq}(O)$.

Data collection: *CrysAlis CCD* (Oxford Diffraction, 2007); cell refinement: *CrysAlis RED* (Oxford Diffraction, 2007); data reduction: *CrysAlis RED*; program(s) used to solve structure: *SHELXS97* (Sheldrick, 2008); program(s) used to refine structure: *SHELXL97* (Sheldrick, 2008); molecular graphics: *XP* in *SHELXTL* (Sheldrick, 2008); software used to prepare material for publication: *SHELXL97*.

References

Allen, F. H. (2002). *Acta Cryst.* B**58**, 380–388.
Bera, A. K., Mukhopadhyay, B. P., Ghosh, S., Bhattacharya, S., Chakraborty, S. & Banerjee, A. (1999). *J. Chem. Crystallogr.* **29**, 531–540.
Berman, H. M., Westbrook, J., Feng, Z., Gilliland, G., Bhat, T. N., Weissig, H., Shindyalov, I. N. & Bourne, P. E. (2000). *Nucleic Acids Res.* **28**, 235–242.
Bhattacharya, S., Bera, A. K., Ghosh, S., Chakraborty, S., Mukhopadhyay, B. P., Pal, A. & Banerjee, A. (2000). *J. Chem. Crystallogr.* **30**, 655–663.
Cremer, D. & Pople, J. A. (1975). *J. Am. Chem. Soc.* **97**, 1354–1358.
Flack, H. D. (1983). *Acta Cryst.* A**39**, 876–881.
Hatzopoulos, G. N., Leonidas, D. D., Kardakaris, R., Kobe, J. & Oikonomakos, N. G. (2005). *FEBS J.* **272**, 3988–4001.
Hoffman, M. M., Khrapov, M. A., Cox, J. C., Yao, J., Tong, L. & Ellington, A. D. (2004). *Nucleic Acids Res.* **32**, D174–D181.
Ishida, T., Doi, M. & Inoue, M. (1988). *Nucleic Acids Res.* **16**, 6175–6190.
Ishida, T., Iyo, H., Ueda, H., Doi, M., Inoue, M., Nishimura, S. & Kitamura, K. (1991). *J. Chem. Soc. Perkin Trans. 1*, pp. 1847–1853.
Leontis, N. B. & Westhof, E. (2001). *RNA*, **7**, 499–512.
Lokanath, N. K., Pampa, K. J., Takio, K. & Kunishima, N. (2008). *J. Mol. Biol.* **375**, 1013–1025.
Luscombe, N. M., Laskowski, R. A. & Thornton, J. M. (2001). *Nucleic Acids Res.* **29**, 2860–2874.
Moodie, S. L. & Thornton, J. M. (1993). *Nucleic Acids Res.* **21**, 1369–1380.
Mukhopadhyay, B. P., Ghosh, S. & Banerjee, A. (1995). *J. Chem. Crystallogr.* **25**, 477–485.
Oxford Diffraction (2007). *CrysAlis CCD* and *CrysAlis RED* in *Xcalibur PX Software.* Version 1.171.32.5. Oxford Diffraction Ltd, Abingdon, England.
Rao, S. T., Westhof, E. & Sundaralingam, M. (1981). *Acta Cryst.* A**37**, 421–425.
Rice, P. A. & Correll, C. C. (2008). Editors. *Protein–Nucleic Acid Interactions: Structural Biology.* Cambridge: RSC Publishing.
Sheldrick, G. M. (2008). *Acta Cryst.* A**64**, 112–122.